Structure, Vol. 9, 699–706, August, 2001, ©2001 Elsevier Science Ltd. All rights reserved. PII S0969-2126(01)00634-7

Structure of the PPARα and -γ Ligand Binding Domain in Complex with AZ 242; Ligand Selectivity and Agonist Activation in the PPAR Family

Philippe Cronet,[1,5] Jens F. W. Petersen,[2,5] Rutger Folmer,[2] Niklas Blomberg,[2] Kristina Sjöblom,[1] Ulla Karlsson,[1] Eva-Lotte Lindstedt,[3] and Krister Bamberg[1,4]

[1] Department of Molecular Biology
[2] Structural Chemistry Laboratory
[3] Department of Medicinal Chemistry
AstraZeneca R&D Mölndal
S-431 83 Mölndal
Sweden

Summary

Background: The peroxisome proliferator-activated receptors (PPAR) are ligand-activated transcription factors belonging to the nuclear receptor family. The roles of PPARα in fatty acid oxidation and PPARγ in adipocyte differentiation and lipid storage have been characterized extensively. PPARs are activated by fatty acids and eicosanoids and are also targets for antidyslipidemic drugs, but the molecular interactions governing ligand selectivity for specific subtypes are unclear due to the lack of a PPARα ligand binding domain structure.

Results: We have solved the crystal structure of the PPARα ligand binding domain (LBD) in complex with the combined PPARα and -γ agonist AZ 242, a novel dihydro cinnamate derivative that is structurally different from thiazolidinediones. In addition, we present the crystal structure of the PPARγ_LBD/AZ 242 complex and provide a rationale for ligand selectivity toward the PPARα and -γ subtypes. Heteronuclear NMR data on PPARα in both the apo form and in complex with AZ 242 shows an overall stabilization of the LBD upon agonist binding. A comparison of the novel PPARα/AZ 242 complex with the PPARγ/AZ 242 complex and previously solved PPARγ structures reveals a conserved hydrogen bonding network between agonists and the AF2 helix.

Conclusions: The complex of PPARα and PPARγ with the dual specificity agonist AZ 242 highlights the conserved interactions required for receptor activation. Together with the NMR data, this suggests a general model for ligand activation in the PPAR family. A comparison of the ligand binding sites reveals a molecular explanation for subtype selectivity and provides a basis for rational drug design.

Introduction

Fatty acids are key components of several metabolic pathways, and organisms have evolved complex mechanisms to maintain a proper balance between absorption, secretion, consumption, and storage of fatty acids. Disorders of lipid metabolism are a major threat to human health, leading to obesity, cardiovascular diseases, insulin resistance, type II diabetes, and atherosclerosis.

Several nuclear receptors, including the peroxisome proliferator-activated receptors (PPARs), control the expression of genes involved in fatty acid metabolism. Three subtypes of PPARs have been identified: α, δ (or β, Nuc-1), and γ, each with specific roles and tissue distribution [1]. In general, PPARα promotes fatty acid catabolism in the liver and skeletal muscle, while PPARγ regulates fatty acid storage in adipose tissues. The physiological role of PPARδ is poorly understood, but a direct link between PPARδ and embryo implantation in the mouse and apoptosis of colon tumor cells has been demonstrated [2, 3]. Similar to the other subtypes, PPARδ binds fatty acids and eicosanoids, suggesting that it is involved in lipid metabolism (see [4] for a recent review). Both PPARα and PPARγ have been demonstrated to be targets for several antidyslipidemic pharmacological agents. Among them, fibrates have been used since the 1960s to lower hypertriglyceridemia and were recently shown to be weak PPARα agonists [5]. PPARγ is activated by several compounds, including the thiazolidinediones (TZDs) [6], a class of compounds used clinically as insulin sensitizers [7] to lower blood glucose in patients with type II diabetes. Both fibrates and TZDs have been shown to lower circulating triglycerides in animal models of hypertriglyceridemia [8].

The structures of the ligand binding domains of human PPARγ [9–11] and human PPARδ [12] have recently been solved in complex with several ligands, providing a structural basis for agonist activation of these subtypes in which the ligand hydrophilic head group plays a key role. However, the general relevance of the activation process remains an open question in the absence of an agonist-bound PPARα_LBD structure. Molecular insight into the interaction of PPARα with a ligand will facilitate the rational design of selective PPAR modulators, which are likely to improve current antidyslipidemic agents.

We present the X-ray structure of the ligand binding domain of human PPARα (here denoted hPPARα_LBD) in complex with AZ 242, a novel compound with combined PPARα and -γ agonist activity that is structurally different than thiazolidinediones. We also report on the conformational differences induced by AZ 242 binding to hPPARα_LBD, as observed by NMR. Based on these data, we propose a general mechanism of ligand-dependent activation that is common to the entire PPAR family, and we provide a molecular explanation for drug selectivity toward the two PPAR subtypes.

Results and Discussion

Activation of PPARα and PPARγ Ligand Binding Domains by AZ 242

AZ 242 is a dihydro cinnamate derivative under development for treatment of insulin resistance-related glucose

[4] Correspondence: krister.bamberg@astrazeneca.com
[5] These authors contributed equally to the work.

Key words: PPAR; agonist; ligand binding domain; structure; NMR; activation

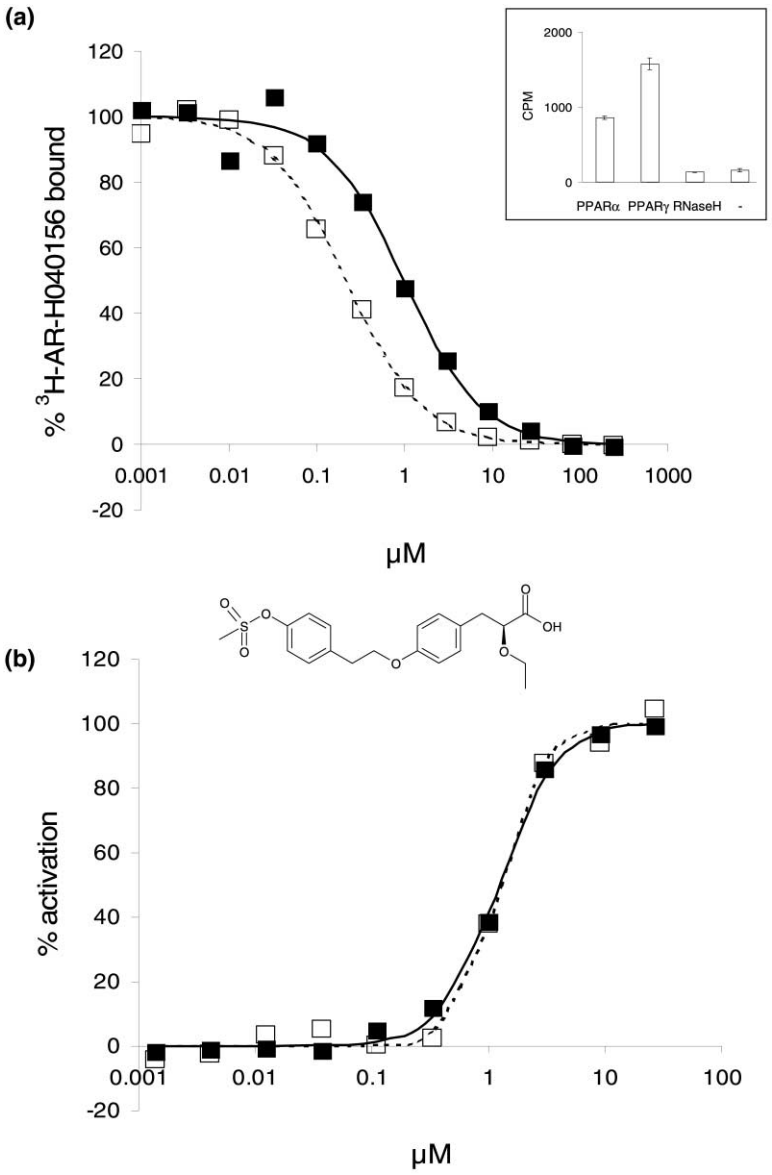

Figure 1. Competition Binding and Coactivator Recruitment of AZ 242

(a) PPARα (solid squares)- or PPARγ (open squares)-bound ^{3}H-AR-H040156 (racemate of AZ 242) was displaced by adding increasing amounts of AZ 242. IC_{50} values for AZ 242 in PPARα and PPARγ were 1.0 μM and 0.2 μM, respectively. The inset figure shows that scintillation from the SPA beads is dependent on the presence of a specific receptor, since the addition of RNaseH to the beads did not increase the counts over background.

(b) AZ 242-mediated coactivator recruitment of SRC-1 peptide to PPARα (solid squares) or PPARγ (open squares) was determined in an in vitro assay based on homogenous time-resolved fluorescence. EC_{50} values for AZ 242 in PPARα and PPARγ were 1.2 μM and 1.3 μM, respectively. The AZ 242 structure is illustrated between the diagrams. XL*fit* (ID Business Solutions) was used to perform curve fitting and IC_{50}/EC_{50} calculations.

and lipid abnormalities associated with type II diabetes and insulin resistance syndrome. A scintillation proximity assay (SPA) was used to determine the binding affinities of AZ 242 toward hPPARα and mPPARγ (Figure 1a). Both receptors bind to the scintillant containing SPA beads by electrostatic interaction, and the dissociation of tritiated AR-H040156 (racemate of AZ 242) is measured at equilibrium without the need for the separation of bound/unbound material. AZ 242 displaces PPARα- and -γ-bound ^{3}H-AR-H040156 with IC_{50} values of 1.0 μM and 0.2 μM, respectively. To demonstrate the agonist nature of AZ 242 on both PPARα and PPARγ, we tested AZ 242 in coactivator recruitment assays based on homogenous time-resolved fluorescence (Figure 1b). AZ 242 led to the recruitment of SRC-1 to both PPARα and PPARγ, with similar ED_{50} values of 1.2 μM and 1.3 μM, respectively. Hence, AZ 242 is an agonist for both PPARα and PPARγ.

General Structural Features

The structure of hPPARα_LBD was solved by molecular replacement and refined including all diffraction data to 2.2 Å (Table 1). The final model consists of one hPPARα_LBD molecule per asymmetric unit. The agonist, AZ 242, the steroid part of a detergent (Deoxy-BIGCHAP [DBC]), and 71 water molecules were included in the final model.

The overall structure of hPPARα_LBD encompasses residues 199–468. Most residues are placed in well-defined electron density, except for two regions, residues 232–234 and residues 254–264, for which no interpretable densities were obtained. Both regions have been left out of the model (Figure 2a). An example of an F_o-F_c electron density omit map calculated around AZ 242 is shown in Figure 2b. The geometry of the final model is good, and no outliers have been found in the Ramachandran plot.

Table 1. Data Collection and Refinement Statistics

Diffraction Data		
Crystal	PPARα/AZ 242	PPARγ/AZ 242
Source	ID14-4	CuKα
Wavelength (Å)	0.9456	1.542
Space group	$P3_121$	C2
Lattice parameters	a = b = 76.9 Å, c = 100.6 Å	a = 92.9 Å, b = 61.8 Å, c = 118.9 Å, and β = 101.5°
Resolution (Å)	20–2.24	20–2.35
Completeness (%)	99.5	91.3
R_{sym}[a] (%)	6.2	6.7
Refinement Statistics		
R_{work}[b] (%)	23.7	23.6
R_{free}[b] (%)	27.1	28.2
Number of Nonhydrogen Atoms Used in Refinement		
Protein	2,064	4,134
Heterogen	53	56
Solvent	71	62
Rmsd bonds (Å)	0.007	0.008
Rmsd angles (°)	1.2	1.2
Average B factor (Å^2)	48.3	51.5

[a] $R_{sym} = \frac{\sum_{hkl}\sum|I(h,k,l,i) - \langle I(h,k,l)\rangle|}{\sum_{hkl}\sum I(h,k,l,i)}$

[b] $R = \frac{\sum_{hkl}||F_{obs}(h,k,l)| - k|F_{calc}(h,k,l)||}{\sum_{hkl}|F_{obs}(h,k,l)|}$

R_{work} is calculated from a set of reflections in which 5% of the total reflections have been randomly omitted from the refinement and used to calculate R_{free}.

The structure of hPPARα_LBD is very similar to both hPPARγ_LBD and hPPARδ_LBD (Figure 2c), with an rmsd between Cα atoms of only 0.9 Å (233 Cα pairs) and 0.8 Å (239 Cα pairs), respectively. A cutoff of 2 Å was used in both cases. The domain consists of 12 helices arranged in an antiparallel helix sandwich. In addition, a 3-stranded antiparallel β sheet is situated in the core of hPPARα_LBD. The largest deviation between the three different crystal structures is found in a region comprising residues 231–265, referred to as the omega loop. This region displays the highest B factors in hPPARα_LBD and differs among the various reported crystal structures of hPPARγ_LBD [9, 11]. Residues 449–457, preceding the C-terminal helix (helix 12 or AF2 helix), constitute a second region exhibiting a large degree of conformational variation between the three subtypes. This segment is more tightly packed onto the core of the domain in PPARα compared with the other two PPAR subtypes.

Crystal contacts with a symmetry-related molecule (symmetry operation: x-y,1-y, 2/3-z) are mediated by the steroid part of the detergent molecule (Figure 2a), explaining the crucial role played by the detergent in the crystallization of hPPARα_LBD. The steroid part is clearly visible in a pocket formed by the N-terminal end of α helices 1 and 8 and the C-terminal end of helix 9, where it forms hydrogen bonds between its axial hydroxyl groups to His411 and Glu451 of the symmetry-related molecule. This is in contrast to the situation observed in hRARγ crystals, in which crystal contacts are formed with a molecule of octyl glucoside occupying the coactivator binding site [13]. The DBC molecule did not interfere with agonist binding in our assays (data not shown), and its mode of binding is probably specific to this crystal form.

Ligand Binding Site

The ligand binding site in hPPARα is located in the central core of the LBD, flanked by helices 3, 5, 7, 11, and 12. It is situated in a large T-shaped cavity similar in size to that of hPPARγ_LBD [9] and hPPARδ_LDB [12], with a volume of about 1300 Å^3. The central cavity spans the domain between the AF2 helix and the 3-stranded antiparallel β sheet. At the level of the β sheet, the cavity splits upward and downward along an axis roughly parallel to helix 3. These extensions are referred to as the upper and lower distal cavities (Figure 2c).

An apparent entrance to the ligand binding site is found between helix 3 and the 3-stranded antiparallel β sheet in a region similar to the proposed entrance in hPPARγ_LBD and hPPARδ_LBD. In the structure presented here, the region from residue 254 to 264 is not included in the model due to poor density. This loop is highly flexible and partly covers the entrance to the ligand binding site. The entrance is further restricted by Tyr334, which forms a hydrogen bond with Glu282. The equivalent residues to Tyr334 in hPPARα_LBD are Glu341 in hPPARγ_LBD, which appears to be flexible [9], and Asn307 in hPPARδ_LBD. Due to these steric hindrances, a great deal of flexibility is probably required in order for large ligands such as AZ 242 to enter the ligand binding site. This is supported by the highly flexible nature of hPPARγ_LBD [14] and hPPARα_LBD, as observed in our NMR experiments.

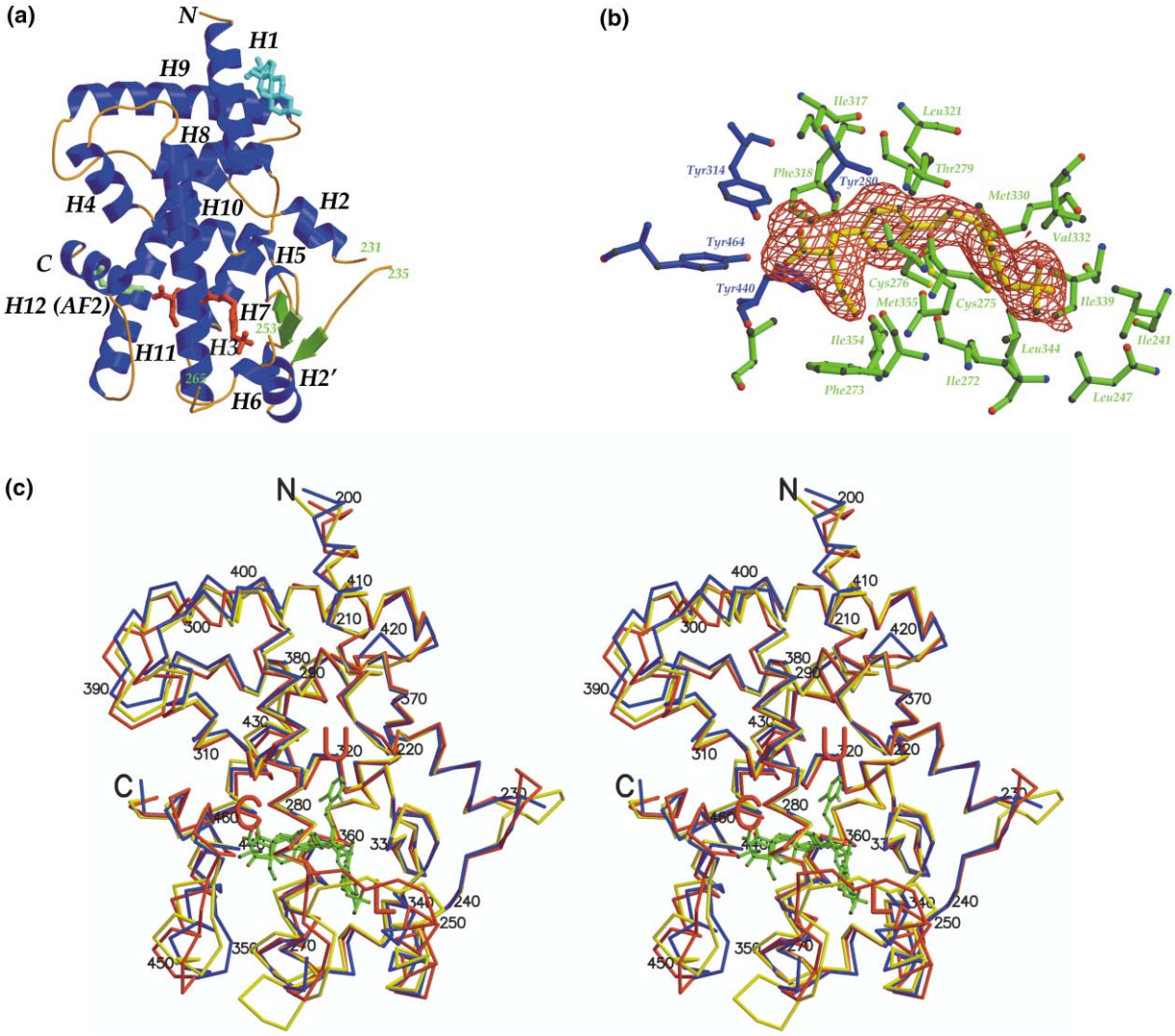

Figure 2. General Structural Features

(a) An overall schematic representation of the hPPARα_LBD structure. The ligand (AZ 242) is shown as a stick model (red). The detergent (DBC) used for crystallization is represented in cyan. The residues immediately adjacent to the regions excluded from the model are indicated by their numbers, and helices are labeled H1–H12. The AF2 helix is labeled.

(b) σA-weighted F_o-F_c electron density omit map calculated around AZ 242. Residues forming hydrophobic contacts with AZ 242 are represented in green, and the residue forming the hydrogen bonds with the propionic head group are represented in blue.

(c) A stereo view of a superposition of hPPARγ_LBD (red) and hPPARδ_LBD (yellow) on hPPARα_LBD (blue). Only the Cα trace is shown. Ligands from the three respective structures are shown in green. The central cavity is marked with a "C", and the upper distal and lower distal cavities are marked with an "U" and "L", respectively.

PPAR Agonism Is Caused by a Conserved Hydrogen Bonding Pattern Involving the AF2 Helix

In all known nuclear receptor crystal structures, the most notable structural differences between apo- and agonist-bound LBD are observed in the C-terminal helix AF2 (e.g., estrogen receptor, PPARγ, RAR). The current model for ligand-dependent activation of nuclear receptors proposes that agonists stabilize a specific conformation of the AF2 helix. Together with helices 3 and 4, the AF2 helix provides a suitable interface for binding a coactivator. In our hPPARα_LBD structure, helices 3, 4, and AF2 exhibit a conformation similar to that observed in other agonist PPAR_LBD complexes, in accordance with the agonist nature of AZ 242.

This situation is also observed with AZ 242 in hPPARγ_LBD. The structure of the AZ 242/ hPPARγ_LBD complex was formed by soaking AZ 242 into crystals of apo-hPPARγ_LBD reproduced from Nolte and collaborators [9]. The crystal form contains two molecules in the assymetric unit, denoted A and B, both containing one AZ 242 molecule. The AF2 helix in the A molecule is in an active state-like conformation, similar to the one observed for the holo-hPPARγ_LBD (PDB accession code 2PRG [9]) as well as in our AZ 242 hPPARα_LBD structure. The AF2 helix in the B molecule does not adopt the active conformation despite the presence of the agonist. Unlike in the A molecule, the AF2 helix in the B molecule forms crystal contacts with a neighboring

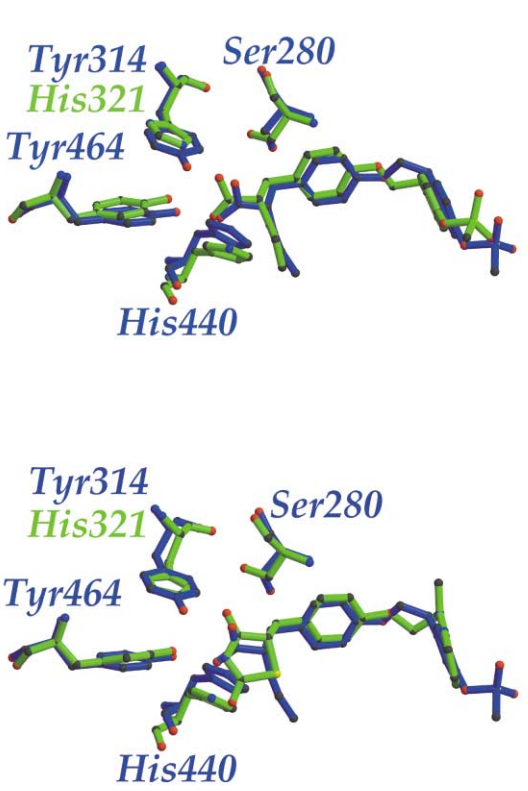

Figure 3. Structural Explanation for the Dual Affinity of AZ 242 to PPARα and -γ

(a) Superposition of the ligand binding sites in hPPARα_LBD (blue) and hPPARγ_LBD (green), both occupied with AZ 242. Only residues that are involved in hydrogen bonding with AZ 242 are shown.

(b) Superposition of the ligand binding site in hPPARα_LBD (blue), occupied by AZ 242, on the ligand binding site in hPPARγ_LBD (green), occupied by rosiglitazone. Only residues that are involved in hydrogen bonding with AZ 242 are shown.

molecule that probably prevent it from moving into the active conformation. We propose that only the A molecule represents a realistic model for the activated PPARγ protein.

Most known PPAR agonists share features such as a hydrophilic head group, a central hydrophobic part, and a flexible linker to the tail. The binding mode of these compounds, AZ 242 included, are highly similar, with the head group interacting with the AF2 helix, the central ring systems forming hydrophobic interactions (Figure 2b), and the tail extending toward the lower or upper distal cavity. The hydrogen bond between the AZ 242 carboxylate group and Tyr464 in the AF2 helix in PPARα and -γ (Figure 3a) is a conserved feature in all agonist PPAR_LBD complexes and has been proposed to directly stabilize the AF2 helix in a conformation that permits coactivator recruitment [10, 12]. The head group of AZ 242 is also hydrogen-bonded to Ser280O^{γ}, Tyr314O^{η} (His321 in PPARγ), and His440$N^{\epsilon 2}$, belonging to helices 3, 5, and 11, respectively, which participate in the coactivator binding site (Figure 3a). This hydrogen bonding network is also present in hPPARδ_LBD [12] and is therefore conserved in the entire PPAR family.

The overall similarity in the binding mode for hPPARα_LBD and hPPARγ_LBD also extends to the coordination of water molecules. A water molecule occupies the same position, in the vicinity of residue 333 and the distal aromatic ring of AZ 242, in both structures. A survey of the available PPAR-ligand complexes in the PDB shows that a water molecule located in this position is also found in 1GWX (PPARδ_LBD in complex with GW2433), 3GWX (PPARδ_LBD in complex with eicosapentanoic acid), and in 2PRG (hPPARγ_LBD in complex with rosiglitazone). Although this water is not involved in any extensive hydrogen bonding network with the protein in any of these structures, it is likely to play an important structural role. These observations support the crucial role of the hydrogen bonding pattern involving the four residues mentioned above for ligand binding and agonist activity in the PPAR family.

A Structural Basis for the Dual Specificity of AZ 242

PPARγ is the molecular target for the thiazolidinedione class of insulin-sensitizing drugs. Thiazolidinediones such as troglitazone, pioglitazone, and rosiglitazone selectively bind PPARγ, compared with the other two PPAR subtypes. In contrast, carboxylic acid-based ligands such as AZ 242 can activate both PPARγ and PPARα. It appears that most of these differences in activity can be attributed to the hydrogen bonding head group. Figure 3b shows a superimposition between the rosiglitazone-hPPARγ and AZ 242-hPPARα hydrogen bonding patterns. Tyr314 in hPPARα_LBD is bulkier than its equivalent in both hPPARγ_LBD (His321) and hPPARδ_LBD (His287; not shown in Figure 3b). We suggest that the carboxylate group in AZ 242 is sufficiently small to form a hydrogen bond with the Tyr314O^{η}, whereas the thiazolidinedione head group is sterically prevented from forming a similar hydrogen bond.

NMR Spectroscopy Shows That the Entire Structure Is Stabilized by Ligand Binding

NMR spectroscopy is a sensitive probe of protein structure and mobility. ^{15}N-edited HSQC spectra probing the environment of the backbone amide protons can be used to monitor protein folding and ligand interactions. Figure 4 shows an overlay of the HSQC spectra in the absence and presence of AZ 242. Several observations can be made from a careful comparison of these two spectra. First, the good dispersion of the crosspeaks and the absence of a high density of resonances around the random-coil chemical-shift positions in the spectrum of the apo-LBD shows that it is well folded, with maybe only a handful of residues in nonstructured regions. Second, a substantial number of crosspeaks move to a significantly different chemical shift upon ligand addition, indicative of substantial conformational changes in the protein. The chemical-shift perturbations are much more marked than would be expected if the ligand merely interacted with some surface residues, hence our conclusion that the protein undergoes a true conformational change. Third, the HSQC spectrum in the presence of a ligand is of higher spectroscopic quality than the spectrum of the apo protein; the lines are

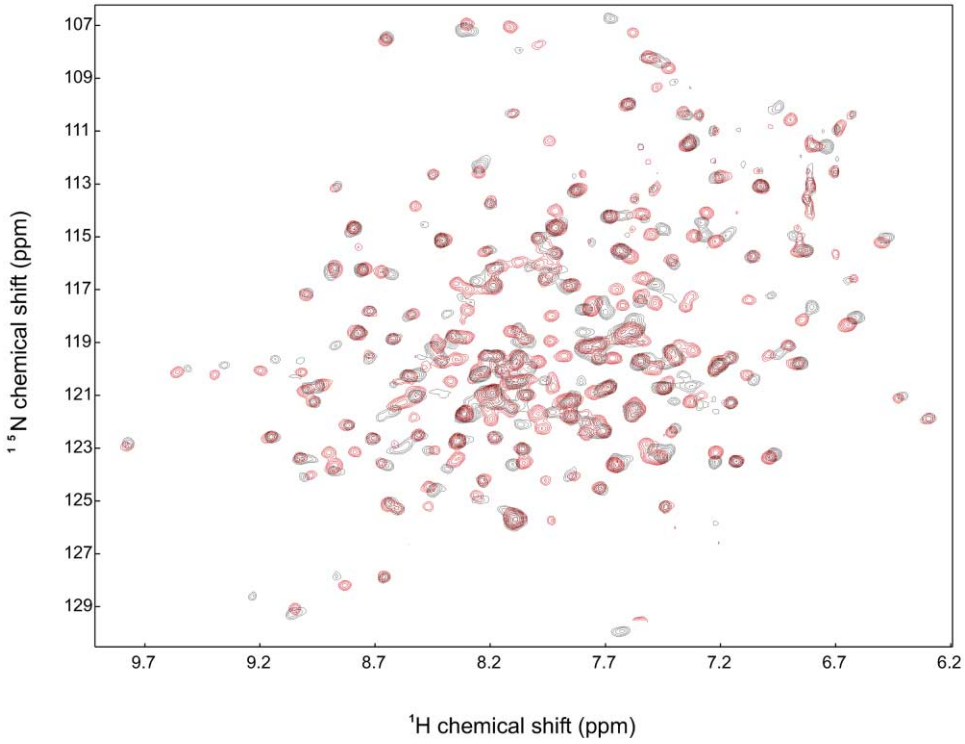

Figure 4. NMR Spectroscopy

An overlay of TROSY HSQC spectra of apo hPPARα_LBD (black) and the protein in complex with AZ 242 (red), recorded at 800 MHz.

narrower, and some 10–20 additional crosspeaks can be identified.

This indicates that the protein adopts a more rigid and defined structure, for which we have two explanations. First, the changes may constitute an overall increase in the "compactness" of the structure, which decreases its overall tumbling time and thereby improves cross-peak line widths. Alternatively, the protein in the absence of ligand may occur partly in multiple conformations, which would lead to line broadening by chemical exchange, causing spectral degradation. Ligand binding would then force the protein to adopt only a single conformation. The two explanations are not completely independent, and both align very well with the common understanding that ligand binding to nuclear receptors directs helices to adopt a defined position with respect to the protein [10, 15]. It is also in line with a recently reported observation that ligand binding in the thyroid hormone receptor stabilizes the hydrophobic core of its LBD [16]. NMR studies on hPPARγ_LBD [14] revealed similar observations; there, a three-dimensional HNCO spectrum of the apo protein reveals less than half of the resonances of that of the rosiglitazone-bound protein and even shows multiple peaks for some of the resonances. The authors conclude that the apo hPPARγ_LBD is in a conformational mobile state, which is frozen into a single conformation by ligand binding. This is similar to our observations for PPARα.

Conclusions

We present the structure of the ligand binding domain from the third member from the PPAR family, PPARα in complex with the dihydrocinnamate derivative AZ 242. The structure reveals extensive similarities to the other subtypes in the architecture of the ligand binding site. The agonist binding mode exhibits a number of conserved features throughout the entire PPAR family. Most of the ligand-protein interactions are hydrophobic, although a conserved hydrogen bonding pattern around the hydrophilic head group of the agonist seems to be important for activity and specificity. One of the residues participating in the hydrogen bonding pattern (Tyr314 in PPARα) differs between PPARα and -δ/γ and seems to play a role in ligand specificity. Moreover, a direct hydrogen bond between the AF2 helix and the hydrophilic head group of the agonist appears to be crucial for maintaining the helix in an adequate conformation for coactivator recruitment.

The NMR data we present here, taken together with the NMR observations on other nuclear receptor ligand binding domains, suggest that nuclear receptors are quite flexible molecules in the absence of a ligand. In addition, the apo structures of PPARγ and PPARδ ligand binding domains suggest that the receptors can adopt the active conformation even in the absence of agonists. All data indicate that the ligand binding domains do not adopt a well-defined structure in the absence of ligands, but instead are in a true equilibrium of conformations.

This indicates a common mechanism of ligand-dependent activation of the PPAR family in which the ligand acts as a skeleton, enabling the PPAR_LBD body to interact with molecular partners. Therefore, ligand binding shifts the protein's conformational equilibrium to a state that favors coactivator recruitment. This model

also predicts that coactivator peptides with high affinity to the receptor could bind to the receptor in the absence of any agonist.

Biological Implications

The peroxisome proliferator-activated receptors (PPARs) are nuclear receptors involved in lipid homeostasis. They have been shown to be activated by fatty acids, eicosanoids, as well as antidyslipidemic drugs. The three described subtypes, PPARα, -δ, and -γ, have specific tissue distributions and are activated by separate ligands in in vitro test systems. Synthetic, small molecule ligands have been described for all three receptors, and PPARα and PPARγ ligands are used clinically as lipid-lowering and insulin-sensitizing drugs, respectively.

The ligand binding domains of the three PPAR subtypes are 60%–65% identical. Given the distinct physiological responses observed for the individual activated receptors, the elucidation of specific ligand-receptor interactions is of great interest. The recently described structures for both PPARγ and PPARδ solved in the presence of specific ligands have provided molecular insights into the binding mode particular for these receptors.

We have performed structural studies on both PPARα and PPARγ ligand binding domains (LBD) in complex with AZ 242, a novel dihydro cinnamate derivative agonist that is structurally different from the thiazolidinediones and has an affinity for both receptors. NMR spectroscopic data obtained from the apo-PPARα and the AZ 242/PPARα complex show a general stabilization of the LBD upon agonist binding. The crystal structures of PPARα and PPARγ in complex with AZ 242 reveal a conserved hydrogen bonding network involving a Tyr in the AF2 helix that must be formed in order to stabilize the LBD in the active conformation throughout the entire PPAR family. A comparison of the ligand binding site allows us to rationalize ligand selectivity toward the α and γ subtypes.

Experimental Procedures

Purification

The ligand binding domains of hPPARα (aa 196–468), hPPARγ (193–475), and mPPARγ (193–475) were expressed as N-terminal His-tagged proteins using a pET28a vector (Novagen). The genes were cloned between the NdeI and BamHI sites. Freshly transformed *E. coli* Bl21DE3 were grown in LB media at 37°C to an OD of 0.6. The culture was induced with 0.1mM IPTG and grown at 18°C for 20 hr. Cells were harvested and resuspended in a 20 ml/L culture of buffer A (20 mM Tris, 150 mM NaCl, 10% glycerol, 1 mM Tris 2-carboxyethyl phosphine HCL (TCEP, Sigma Aldrich) [pH8]). The cells were disrupted by sonication in the presence of protease inhibitors (Complete EDTA-free, Roche), and the soluble fraction was isolated by centrifugation (35,000×g, 45 min). The pH of the supernatant was checked, and the supernatant was loaded onto Ni-NTA (1 ml/L culture) and eluted with a gradient imidazole 0–300 mM over 20 column volumes of buffer A. The fractions containing the protein were dialyzed over buffer A to remove imidazole, and the protein was cleaved with thrombin protease (10 U/mg) at room temperature until completion, a process that was monitored by ES-MS. The His tag and uncleaved material were removed by incubation with Ni-NTA. The flow through was diluted with buffer B (20 mM Tris, 10% glycerol, 1 mM TCEP [pH8]) to 20 mM NaCl and immediately loaded onto a Q sepharose HP column (Amersham-Pharmacia Biotech). The protein was eluted with a gradient to 100% buffer B supplied with 500 mM NaCl over 20 column volumes. The protein was then concentrated, desalted against buffer A, and frozen in 2 ml aliquots at a concentration of 1 mg/ml.

^{15}N labeling of the protein was performed in a medium containing 3/4 M9 minimal medium supplemented with 1/4 Martek ^{15}N-labeled Celtone. The purification was performed using the same method as for the nonlabeled protein.

Competition Binding

A scintillation proximity assay (SPA) was used to determine binding affinities of AZ 242 for hPPARα and mPPARγ. The reactions were performed in 100 μl buffer containing 20 mM Tris (pH 7.5), 80 mM NaCl, 2 mM TCEP, 0.125% CHAPS, and 10 % glycerol. Each well contained 0.1 mg polylysine-coated yttrium silicate beads (Amersham Pharmacia Biotech), 150 nM PPARα or PPARγ, respectively, and 250 nM ^{3}H-AR-H040156 (racemate of AZ 242, 1.12×10^{15} Bq/mol). AZ 242 was added without preincubation. All components were mixed and incubated while gently shaking for 1 hr at room temperature. Scintillation counts were determined in a Wallach Trilux (Wallach).

Coactivator Recruitment

The activity of recombinant hPPARα and mPPARγ was confirmed in a coactivator recruitment assay. Eu^{3+}-coupled anti-His antibody (anti-His-Eu^{3+}) and APC-coupled streptavidin (SA-APC) were obtained from Wallach. An N-terminally biotinylated 24-amino acid peptide (Innovagen AB) derived from SRC-1 was used as a coactivator (NH_2-CPSSHSSLTERHKILHRLLQEGSPS-COOH). A 45-μl reaction volume contained 20 mM Tris (pH 7.5), 0.5 μM NaCl, 2 mM DTT, 0.05% BSA, 6.8 ng anti-His-Eu^{3+}, and 360 ng SA-APC. The PPARα assay contained 800 nM hPPARα_LBD and 1200 nM biotinylated SRC-1 peptide; the PPARγ assay contained 600 nM mPPARγ_LBD and 800 nM SRC-1 peptide. After the addition of all reagents, plates were incubated for 1.5 hr at room temperature, and time-resolved fluorescence was measured in a Victor2 (Wallach). Excitation was at 340 nm, and fluorescence was measured at 620 nm and 665 nm. Specific signals were calculated by dividing the 665 nm signal by the 620 nm signal and multiplying the fraction by 10,000.

Compounds

The synthesis of the dihydro cinnamate derivative AZ 242 ((*S*)-2-ethoxy-3-[4-[2-(4-methylsulfonyloxyphenyl)ethoxy]phenyl]propanoic acid) was as described (Andersson, K. January 2001. Sweden, patent WO 9962872). The radiolabeled racemic mixture AR-H040156 was obtained by reacting an unsaturated precursor with tritium gas. Radiochemical purity was 99%, as determined by HPLC.

Crystallization

The protein was concentrated to 7 mg/ml (20 mM Tris, 150 mM NaCl, 10% glycerol, 1 mM TCEP [pH8]). The ligand AZ 242 was added to a final concentration of 0.5 mM, and Deoxy Big CHAP (DBC) was added to a concentration of 0.7 mM. The solution was mixed to an equal volume of 3.2 M Na Formate, HEPES 100 mM (pH7.5) and crystallized using hanging drop-vapor diffusion at 293K. Crystals appeared after 7–10 days. Crystals of apo-hPPARγ_LBD were prepared as previously described [9]. Pure AZ 242 was added to the crystal in the mother liquor and left to equilibrate for 2–3 weeks.

Structure Determination and Refinement

Crystals of hPPARα_LBD were transferred into cryoprotectant solution (mother liquor + 30% v/v glycerol) and immediately thereafter flash frozen at 100K. The data sets were collected at beam line ID14-4 at the ESRF Grenoble on a Quntam4 CCD detector. The images were indexed and integrated using Mosflm [17] and further processed using SCALA and TRUNCATE from the CCP4 program package [18] (merging statistics are shown in Table 1). The structure of hPPARα_LBD was solved by molecular replacement using EPMR [19]. The structure of apo-hPPARγ_LBD [9] was used as a search model. The model of hPPARα_LBD was built using TURBO-FRODO [20] and refined using simulated annealing and individually restrained B factor refinement included in CNX [21]. Both bulk solvent

correction and anisotropic B factor scaling were applied. The geometry of the final model was validated using WHAT-IF CHECK [22].

Diffraction data on the hPPARγ_LBD/AZ 242 complex crystal were collected on a Rigaku Rotaflex rotating anode equipped with Osmic mirrors, using a MAR345 image plate detector. The crystals were flash frozen directly from the mother liquor at 100K. The diffraction data were indexed, integrated, and scaled using DENZO and SCALEPACK from the HKL suite [23]. Model building was performed using TURBO-FRODO, and the models were refined using simulated annealing and restrained B factor refinement included in CNX. The geometry of the final model was validated using WHAT-IF CHECK.

NMR

NMR samples contained 200–300 μM ^{15}N-labeled protein in a buffer consisting of 40 mM Tris (pH 7.5), 150 mM NaCl, 1 mM TCEP, and 5% glycerol. ^{15}N HSQC experiments were recorded as TROSY spectra [24, 25] on a Bruker DRX800 at 293K. Typical acquisition times were 30–90 min. Although the sensitivity of the TROSY experiments was slightly less than that of a conventional HSQC, it was still the experiment of choice because of the drastic line width reduction. Spectra were analyzed with NMRview [26].

Acknowledgments

We want to thank Roger Simonsson for providing tritiated ligand, Sean McSwenny at the ESRF for technical assistance, and the AstraZeneca Biotech Lab-Södertälje for the large scale protein production. The authors wish to thank Mikael Dohlsten, David Rees, Nigel Darby, Bengt Ljung, Per Falk, and Gill Bishop for critically reading the manuscript.

Received: April 4, 2001
Revised: June 7, 2001
Accepted: July 9, 2001

References

1. Michalik, L., and Wahli, W. (1999). Peroxisome proliferator activated receptors: three isoforms for a multitude of functions. Curr. Opin. Biotech. *10*, 564–570.
2. He, T.C., Chan, T.A., Vogelstein, B., and Kinzler, K.W. (1999). PPARδ is an APC-regulated target of nonsteroidal antiinflamatory drugs. Cell *99*, 335–345.
3. Lim, H., et al., and Dey, S.K. (1999). Cyclo-oxygenase-2-derived prostacyclin mediates embryo implantation in the mouse via PPARδ. Genes Dev. *13*, 1561–1574.
4. Willson, T.M., Brown, P.J., Sternbach, D.D., and Henke, B.R. (2000). The PPARs: from orphan receptors to drug discovery. J. Med. Chem. *43*, 527–550.
5. Issemann, I., Prince, R.A., Tugwood, J.D., and Green, S. (1993). The peroxisome proliferator-activated receptor:retinoid X receptor heterodimer is activated by fatty acids and fibrate hypolipidaemic drugs. J. Mol. Endocrinol. *11*, 37–47.
6. Lehmann, J., et al., and Kliewer, S.A. (1995). An antidiabetic thiazolidinedione is a high affinity ligand for peroxisome proliferator-activated receptor (PPAR). J. Biol. Chem. *270*, 12953–12956.
7. Schoonjans, K., and Auwerx, J. (2000). Thiazolidinediones: an update. Lancet *355*, 1008–1010.
8. Lefebvre, A., et al., and Staels, B. (1997). Regulation of lipoprotein metabolism by thiazolidinediones occurs through a distinct but complementary mechanism relative to fibrates. Arterioscler. Thromb. Vasc. *17*, 1756–1764.
9. Nolte, R.T., et al., and Milburn, M.V. (1998). Ligand binding and co-activator assembly of the peroxisome proliferator-activated receptor. Nature *395*, 137–143.
10. Gampe, R.T., et al., and Xu, H.E. (2000). Asymmetry in the PPARγ/RXRα crystal structure reveals the molecular basis of heterodimerization among nuclear receptors. Mol. Cell *5*, 545–555.
11. Uppenberg, J., et al., and Berkenstam, A. (1998). Crystal structure of the ligand binding domain of the human nuclear receptor PPARγ. J. Biol. Chem. *273*, 31108–31112.
12. Xu, H.E., et al., and Milburn, M.V. (1999). Molecular recognition of fatty acids by peroxisome proliferator-activated receptors. Mol. Cell *3*, 397–403.
13. Klaholz, B.P., and Moras, D. (2000). Structural role of a detergent molecule in retinoic acid nuclear receptor crystals. Acta Crystallogr. D *56*, 933–935.
14. Johnson, B.A., et al., and Zhou, G. (2000). Ligand induced stabilisation of PPARγ monitored by NMR spectroscopy: implications for nuclear receptor activation. J. Mol. Biol. *298*, 187–194.
15. Renaud, J.P., et al., and Moras, D. (1995). Crystal structure of RAR-γ ligand binding domain bound to all-trans retinoic acid. Nature *378*, 681–689.
16. Pissios, P., Tzameli, I., Kushner, P., and Moore, D.D. (2000). Dynamic stabilization of nuclear receptor ligand binding domains by hormone or corepressor binding. Mol. Cell *6*, 245–253.
17. Leslie, A.G.W. (1990). Molecular Data Processing, (Oxford: Oxford University Press).
18. Collaborative Computational Project No. 4. (1994). The CCP4 suite: programs for protein crystallography. Acta Crystallogr. D *50*, 760–763.
19. Kissinger, C.R., Gehlhaar, D.K., and Fogel, D.B. (1999). Rapid automated molecular replacement by evolutionary search. Acta Crystallogr. D *55*, 484–491.
20. Roussel, A., and Cambillau, C. (1992). TURBO-FRODO. In Silicon Graphics Geometry Directory. (Mountain View, CA: Silicon Graphics), p. 86.
21. Brunger, A.T., et al., and Warren, G.L. (1998). Crystallography & NMR system. Acta Crystallogr. D *54*, 905–921.
22. Hooft, R.W.W., Vriend, G., Sander, C., and Abola, E.E. (1996). Errors in protein structures. Nature *381*, 272.
23. Otwinoski, Z., and Minor, W. (1997). Processing of X-ray diffraction data collected in oscillation mode. Methods Enzymol. *277*, 307–325.
24. Pervushin, K., Riek, R., Wider, G., and Wuthrich, K. (1997). Attenuated T-2 relaxation by mutual cancellation of dipole-dipole coupling and chemical shift anisotropy indicates an avenue to NMR structures of very large biological macromolecules in solution. Proc. Nat. Acad. Sci. USA *94*, 12366–12371.
25. Czisch, M., and Boelens, R. (1998). Sensitivity enhancement in the TROSY experiment. J. Magn. Reson. *134*, 158–160.
26. Johnson, B.A., and Blevins, R.A. (1994). NMRView: a computer program for the visualisation and analysis of NMR data. J. Biomol. NMR *4*, 603–614.

Accession Numbers

The PPARα and PPARγ coordinates have been deposited in the Protein Data Bank with PDB IDs 1I7G and 1I7I, respectively.

Note Added in Proof

During the preparation of this manuscript, Oliver, et al. [Oliver, W.R., Jr. et al., and Willson, T.M. (2001). A selective peroxisom proliferator-activated receptor delta agonist promotes reverse cholesterol transport. Proc. Natl. Acad. Sci. USA *98*, 5306–5311] have used a PPARδ-selective agonist to demonstrate a role for PPARδ in cholesterol metabolism.